Study of Crystallization of Low Molecular Mass Poly(ethylene oxide) from the Melt†

Stephen Z. D. Cheng

Institute and Department of Polymer Science, University of Akron, Akron, Ohio 44325

Bernhard Wunderlich*

Chemistry Division, Oak Ridge National Laboratory, Oak Ridge, Tennessee 38731-6197, and Department of Chemistry, University of Tennessee, Knoxville, Tennessee 37996-1600.
Received April 15, 1988; Revised Manuscript Received September 16, 1988

ABSTRACT: A study is made to clarify mass-dependent crystallization kinetics and to connect it to the observed rejection of low molecular mass species. The concepts of molecular nucleation, perfection during nucleation, and cooperative crystal growth kinetics are discussed. Poly(ethylene oxide) is the example macromolecule.

Introduction

About 15 years ago it was suggested that molecular nucleation and not secondary nucleation may be the rate-determining step in crystal growth of macromolecules. This suggestion was based on an experimental study of the segregation of low molecular mass polyethylene (PE) from crystals of high molecular mass grown from melt or solution using a polymer sample of broad molecular mass distribution.[1-3] In short, it was observed that virtually complete segregation of molecules was possible *below* the equilibrium and zero-entropy-production melting temperatures. Since in the framework of standard crystal growth models only at these equilibria (and not below) reversibility in the presence of a suitable surface should be guaranteed for each molecule, it was necessary to introduce a new, molecular nucleation barrier. This is in addition to the well-documented primary and secondary crystal nucleation barriers that cannot act on every molecule but only once per nucleation event. More recently we reported such segregation for a second polymer, poly(ethylene oxide) (PEO), crystallized from the melt. In this latter case various low and high molecular mass fractions were mixed in the melt, and their degree of segregation on crystallization was analyzed. The detailed study of segregation included calorimetry,[4] kinetic measurement,[5] and morphological observations.[6] Computer simulation of the process is being developed.[7] In the present study we search for a more detailed description of crystallization and segregation based on the extensive data for PEO. The kinetics of crystallization of PEO fractions and binary mixtures is known better than that of any other polymer.[5,8-12] In addition, the thermodynamics of the system is solidly backed by experiment. Heat capacities for crystals, glass, and melt are known for all temperatures.[13-15] Equilibrium melting temperatures, $T_m(0)$, are known as a function of mass, and zero-entropy-production melting temperatures, $T_m(m)$, are known as a function of mass and number of chain folds, m, per molecule.[16] The zero-entropy-production melting temperature of an m-times folded molecule is of particular importance since it takes the place of the equilibrium melting temperature when discussing phase equilibria of crystals of chain-folded molecules. Heats of fusion are similarly well established for equilibrium and nonequilibrium crystals.[16] The crystal structure, morphology, and macroconformation of PEO crystallized from solution and melt have also been extensively studied.[6,8-12] All these experiments provide a unique resource for the discussion of crystallization.

† This work is based on experimental work carried out by both authors at Rensselaer Polytechnic Institute.

The Status of the Understanding of Crystallization of Macromolecules

Theories of polymer crystal growth developed over the past 30 years rely solely on the assumption that surface free energy effects hinder quick crystallization. Many authors have developed these theories[17-20] so that they may now be called "classic".[21]

In more detail, classical crystal growth at low supercooling is assumed to proceed as follows:[22] A crystal layer of single molecular thickness b and average fold length l grows with a speed v_g (length/time) parallel to the surface and stops after reaching an average width L when it meets an obstacle that is capable of interrupting layer completion. The nucleation rate of the layers i is expressed in nuclei/(area × time). On the basis of this simple model three crystallization regimes were identified.[23-27] (Note that these three regimes of crystallization must not be confused with the three temperature regions of different degree of segregation discussed below.[4,5]) For regimes I and III the overall, linear crystal growth rate v_c in length/time normal to the crystal surface is proportional to biL. For regime II the linear crystal growth rate v_c is proportional to $b(2v_g i)^{1/2}$. With the further assumption of one step of length l being crystallized at a time, chain-folding with adjacent reentry and molecularly smooth crystal surfaces can be described.[25-27] Figure 1, below, indicates as was observed earlier by Kovacs that the suggested change of v_c with temperature for regimes I, II, and III is not realized for PEO. Point and Kovacs[28] have shown that the experimental v_c for low molecular mass fractions at low supercooling may reach values 8 orders of magnitude larger than expected from the classical theory.

In a more recent treatment, Hoffman[29] suggested that this largely different crystallization behavior of low molecular mass PEO can be fitted to the classical crystallization theory by assuming a continuous increase of lamellar thickness with crystallization temperature T_c, placing the observed low-supercooling crystallization kinetics into regime III, and introducing an average fold surface free energy. The observed, stepwise increase of lamellar thickness must then be caused by secondary, isothermal, lamellar thickening; the regime III kinetics that was originally postulated for low T_c must now be used at high T_c; and the fold-surface free energy that is known from melting experiments to vary with fold number m must assume a different behavior for crystallization.

Another attempt at describing low molecular mass PEO crystallization rates was made by Sadler based on the hypothesis of molecularly rough crystal surfaces.[30] A

0024-9297/89/2222-1866$01.50/0

continuous crystal growth without need for surface nucleation would then take place. A linear relationship between v_c and T_c is under these conditions expected and has been verified by computer simulation. Experimentally v_c is, however, for low molecular mass fractions not linear at low supercooling. This was recognized by Sadler as the so-called "tail problem" and was suggested to be due to segregation. Surface nucleation is also proven to exist in many cases on the morphological evidence of rare starts of crystal overgrowth on extended-chain crystals.[31]

All of these attempts to account for the crystal growth do not yield the proper functional mass dependence of v_c and cannot explain full segregation of low-mass molecules below their equilibrium or zero-entropy-production melting temperatures $T_m(m)$.

In this paper we analyze crystallization experiments on the assumptions that there must be a molecular nucleus before a molecule can commence to crystallize; that crystal perfection occurs not only after crystallization but also during crystallization and even nucleation; and that there is cooperativity, i.e., there exists an effect of lamellar thickness and molecular length on v_c in addition to any effect of surface free energy barriers.

Experimental Evidence for Molecular Mass Dependent Nucleation Barriers

According to the concept of molecular nucleation, reversible polymer crystal growth and melting can occur only as long as a single macromolecule is partially crystallized and the crystallized portion of the molecule is equal to or larger than the molecular nucleus.[3] To add a new molecule to a crystal, a molecular nucleation step is necessary. One must thus separate crystal nucleation and molecular nucleation.

At low supercooling for sufficiently large macromolecules all nucleation can occur on a one-molecule scale. As molecular mass decreases, more than one molecule may become involved in nucleation, ultimately leading to the well-known primary and surface nucleation observed for crystals of small molecules. For the growth of macromolecular crystals there is thus, because of the need for molecular nucleation, a certain supercooling range where practically no growth occurs, even in contact with primary and surface nuclei. A macromolecular melt in this temperature range is metastable.

Experimentally this range of metastability was first documented by the failure to be able to seed PE melt with equilibrium, extended-chain, rough-surface crystals of the same chemical nature.[32] More quantitative data on the linear crystallization and melting rate are available for PEO (Figure 3 of ref 5), PE (Figure 9b of ref 33), and Se (Figure 1 of ref 3 and Figure 6 of ref 34). All three examples show that only on extrapolating of the molecule size to monomer dimensions is there continuity between crystal growth and melting at the melting temperature. Based on these observations alone there must be a free enthalpy barrier for the crystallization of each and every molecule (molecular nucleation). The need for nucleation to initiate a crystal (primary nucleation, heterogeneous in most cases) and often also a new layer on a molecularly smooth crystal surface (secondary or surface nucleation) is proven largely by morphological evidence.[21,31] Using crystallization kinetics, a molecular nucleus may be difficult to distinguish from a surface nucleus. Except for its much more limited effect on crystal morphology, one can perhaps use almost identical mathematical representations for surface and molecular nucleation as was proposed in ref 1. After molecular nucleation, crystal growth stops not later than with the complete crystallization of the given molecule; i.e., L has an upper limit set by the length of the molecule. Recent estimates from kinetic evidence of the length of L that one surface nucleus causes the growth of 5–25 macromolemolecules of 100 000 molecular mass[35a,b] underscore the need for additional molecular nucleation. If surface nucleation were the process responsible for rejection of too short molecules it could be effective only one out of 5–25 times and not practically for every molecule.

Turning to the molecular mass dependence of linear crystal growth, it was shown that PEO and five other macromolecules satisfy the following relationships, which is close to an earlier suggestion of Magill's (private communication to us of unpublished data after publication of ref 5):[5]

$$\log v_c = A \log [\ln (n)] + B \quad (1)$$

$$0.434\Delta G_n/(kT) = -A \log [\ln (n)] \quad (2)$$

where n is the degree of polymerization of the crystallizing molecule, k is the Boltzmann constant, and A and B are constants linked to the experimentally available linear crystal growth rate v_c. The molecular mass dependent part of the free enthalpy barrier to crystallization is ΔG_n. The molecular mass independent part of the free enthalpy barrier is contained within B. Both, A and B can vary with the degree of supercooling $\Delta T = T_m(m) - T_c$. Data for A and B of PEO are listed in Table I for a wide range of ΔT. Insertion of A and B in eq 1 leads to a v_c in nm/s.

Table I
Molecular Mass Dependent and Independent Nucleation Barriers for PEO Crystals of Integral Folding and Nonintegral Folding

ΔT,[a] K	$-A$	B, nm/s	ΔT,[a] K	$-A$	B, nm/s
	$m = 0$			$m = 3$	
0.5[b]	23.4[b]	12.5[b]	0.5[b]	33.3[b]	27.0[b]
1.0	24.2	14.0	1.0	30.0	21.0
1.5	25.1	15.3	1.5	27.6	19.6
2.0	25.8	16.2	2.0	26.0	18.9
2.5	26.5	16.9	2.5	25.8	18.8
3.0	27.2	17.7	3.0	26.4	19.7
3.5	27.9	18.3	3.5	27.5	20.8
4.0	28.7	18.8	4.0	28.9	22.0
4.5	29.4	19.3	4.5	31.8	24.3
5.0	30.1	19.8			
5.5	31.0	20.4	m: Nonintegral Folding		
			6.0[c]	6.14	5.67
	$m = 1$		8.0[c]	5.58	5.88
0.25[b]	30.2[b]	18.3[b]	10.0[c]	5.06	6.06
0.5	27.3	17.2	12.5	4.56	6.21
1.0	25.9	17.0	15.0	4.02	6.33
1.5	27.6	18.7	17.5	3.58	6.48
2.0	30.0	20.7	20.0	3.06	6.53
2.5	31.6	22.0	22.5	2.79	6.53
3.0	32.9	23.1	25.0	2.38	6.40
3.5	34.0	24.0	27.5	2.10	6.31
4.0	34.9	24.8	30.0	1.72	6.15
	$m = 2$				
0.5[b]	28.4[b]	18.9[b]			
1.0	25.9	17.8			
1.5	25.3	17.7			
2.0	25.8	18.4			
2.5	27.1	19.5			
3.0	28.1	20.5			
3.5	29.4	21.8			
4.0	30.9	23.3			

[a] The supercooling for crystals of integral folding is defined as $T_m(m) - T_c$, the effective supercooling. The supercooling for crystals of nonintegral folding is defined as $T_m^0 - T_c$ (T_m^0, the equilibrium melting temperature of infinite molecular mass is 342.1 K or 68.9 °C). [b] Data based on extrapolated crystal growth rates. [c] Data in the supercooling range of 6–10 K for nonintegral folding could only be derived from the crystal growth rate of high molecular mass molecules (MW = 17 500, 100 000, 152 000, and 5 000 000).

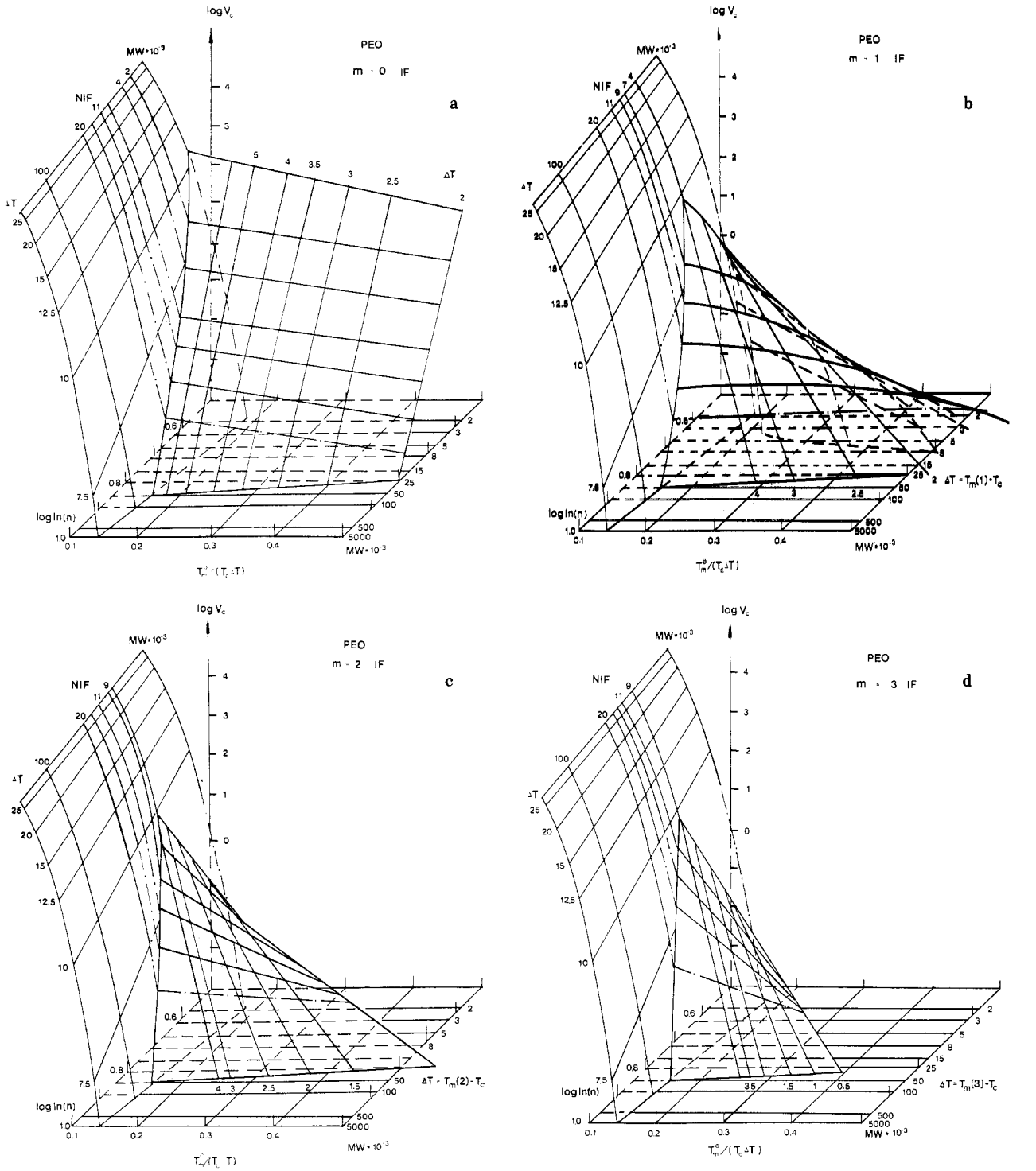

Figure 1. Linear growth rates v_c of crystals with nonintegral (NIF) and integral (IF) folds as function of molecular mass MW and supercooling ΔT in nm/s. Coordinates are given as log v_c, log [ln (n)], and $T_m/(T_c\Delta T)$ where m represents the number of folds and n the degree of polymerization. The IF crystals correspond to m = 0, 1, 2, and 3 in (a)–(d), respectively.

When considering cooperative models (added on suggestion of the reviewer of this paper), power laws are more often observed than logarithmic expressions as in eq 1. Assuming, n^γ expresses the molecular mass dependence of a cooperative process, one can via $n^\gamma = (e^{\ln n})^\gamma = e^{\gamma \ln n}$ express n^γ approximately as $1 + \gamma \ln n$ if γ is small. Equation 1 would then take the form

$$v_c = v_0 + Kn^\gamma \qquad (1a)$$

An attempt to represent the correlation between v_c, $1/\Delta T$, and molecular mass MW is shown in Figure 1. Extensive crystal growth rate data have been collected for this figure on 17 PEO fractions. Seven data sets were measured by Kovacs et al.[8-12] (MW of 1890, 2780, 3900, 5970, 7760, 9970, and 152000) and 10 by us[5,36] (MW of 950, 1400, 3500, 4640, 7000, 9230, 11250, 17500, 100000, and 5000000). The v_c surface for nonintegrally folded crystals (NIF) is the same for parts a and d of Figure 1. It is intersected by the v_c surfaces for the integrally folded crystals (IF) with 0, 1, 2, and 3 folds per molecule for parts a–d of Figure 1, respectively. The change from NIF to IF depends on ΔT and MW. All boundaries of Figure 1a–d approach each other on extrapolation to low supercooling and high molecular mass (lower left corners of the figure). The approximate intersection point occurs at MW = 50000, $v_c = 10^{-4}$ nm/s, and ΔT = 6 K.

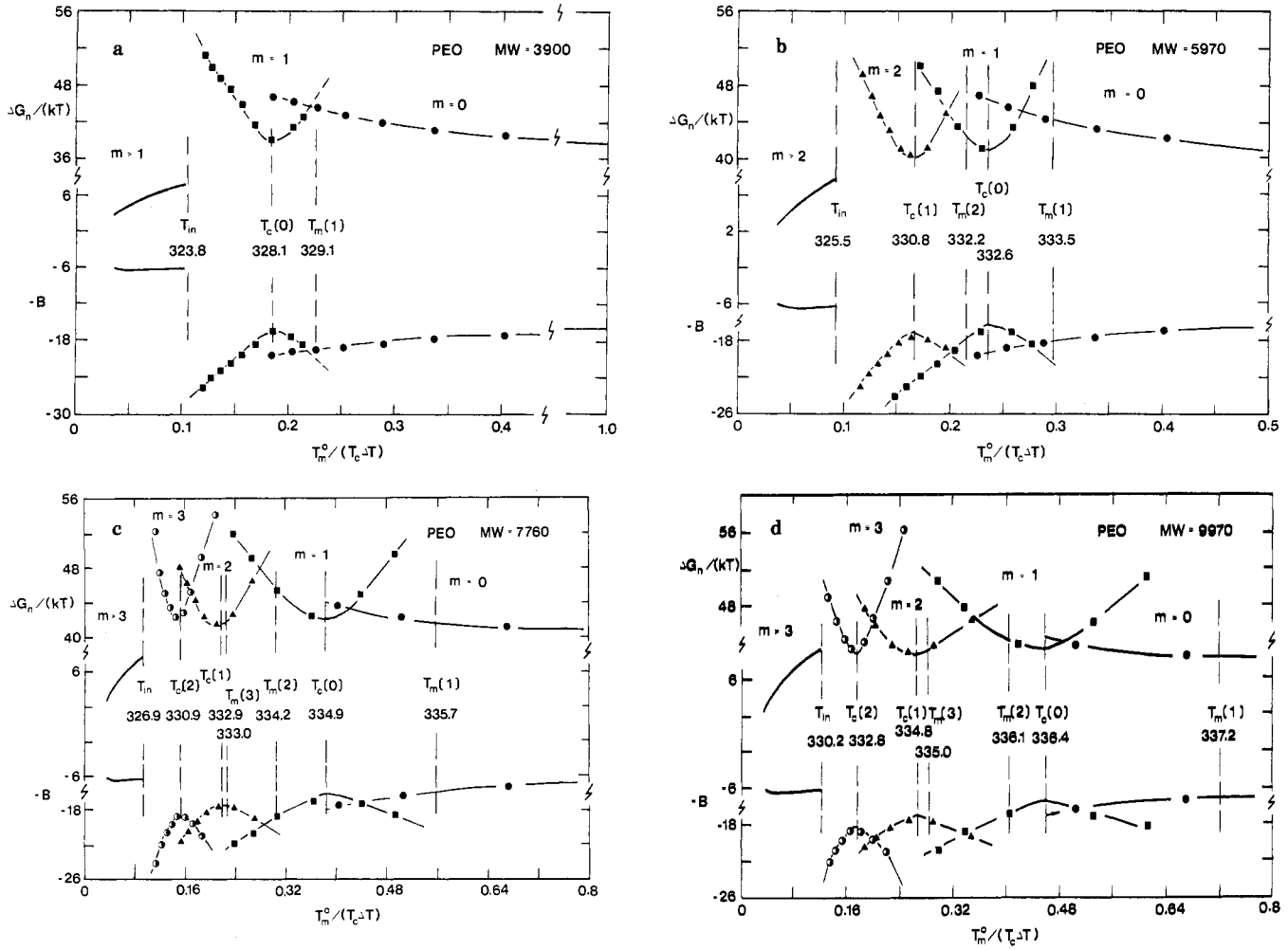

Figure 2. Molecular mass dependent and independent parts of the nucleation barrier for low molecular mass fractions [$\Delta G_n/(kT)$ and $-B$, respectively] as a function of the inverse of supercooling. Points are the experimental values of Kovacs et al.,[8-12] B in nm/s.

In the high supercooling range, a single NIF surface describes crystal growth and increasing ΔT produces a continuously increasing A, while B changes little (see Table I). Since eq 2 holds for the whole range of masses, one can assume that there is no basic change in crystal growth mechanism with molecular mass on this surface.

In the low supercooling range integral folding (IF) becomes possible, with each fold number m corresponding to a different v_c surface, indicating the existence of specific crystal growth paths. Using the same treatment of the growth rate as for the high supercooling range one can draw the corresponding curves for $\Delta G_n/(kT)$ and B as a function of $T_m(0)/(T_c\Delta T)$ as shown in Figure 2 for four examples.

For any m, $\Delta G_n/(kT)$ decreases at first with decreasing ΔT, in contrast to the NIF crystals which show always a continuous increase. The NIF data are shown for comparison on the left-hand sides of the figure. For IF crystals with $m > 1$, $\Delta G_n/(kT)$ reaches a minimum followed by an almost symmetric increase at even lower ΔT. That there is no minimum for $m = 0$ could be verified to a ΔT value of as little as 1 K. The molecular mass independent term B shows a systematic correspondence to $\Delta G_n/(kT)$ (see also Table I), so that the appropriate sum satisfies eq 1 and Figure 1.

Several characteristic temperatures are marked in Figure 2. The lowest, T_{in}, marks the temperature of change from high-supercooling NIF crystallization to IF crystallization, it occurs at 323.8, 325.5, 326.9, and 330.2 K for parts a–d Figure 2, respectively. Next are the temperatures of the minima in the $\Delta G_n/(kT)$ curves and the corresponding maxima in the B curves. They occur close to the temperatures where for the first time growth of crystals with $(m - 1)$ folds occurs, $T_c(m - 1)$. For example, in Figure 2a the minimum in $\Delta G_n/(kT)$ occurs at 328.1 K, at $T_c(0)$, the first crystallization temperature of extended-chain crystals. Similarly, in Figure 2b the minima for $m = 1$ and $m = 2$ are at 329.5 and 332.1 K, close to the marked $T_c(1)$ and $T_c(0)$. Finally, the points of intersection of $\Delta G_n/(kT)$ for crystals of m and $(m - 1)$ folds, T_c^*, is always located between $T_m(m)$ and $T_c(m - 1)$.

The absolute values of the various characteristic crystallization and melting temperatures can be used to get information on nucleus and crystal stability. Local equilibrium for the molecular nucleus is reached when ΔG is zero, i.e., when the nucleation barrier has been surmounted and the free enthalpies of nucleus and melt are equal. At this point one expects local reversibility of the nucleation process to be active. This reversibility is needed for the rejection of species of insufficient length, to be discussed in the next section (see also Figure 4). Morphological evidence on PEO[8] and calorimetry on PE[32] have proven that perfection is a continuous process on crystallization. It may thus occur during nucleation as well as during and after crystal growth. At $T_c(m - 1)$ the perfection due to unfolding of an m-times folded molecule on a substrate thick enough to accommodate $(m - 1)$ folds reaches the rate of formation of an m-times folded nucleus; i.e., an $(m - 1)$-times folded crystal can grow directly from this temperature on when properly crystal nucleated. The

Table II
Molecular Segregation Parameters

MW	T_c^*(I,II)[a]	T_c^*[b]	$T_c(0)$[c]	$T_c(1)$[c]	$T_c(2)$[c]	no. of folds[d]	l_c[d]	l[e]
3500	330.4	328.4	327.8			0	22.1	24.1
4640	331.2	331.2	330.7			1 - 0	14.7-29.3	25.1
7000	334.0	334.0	333.6	331.7	327.5	1 - 0	22.1-44.2	28.1
9230	334.5	334.5	335.4	333.7	331.9	2 - 1	19.5-29.2	28.6
11250	334.9	335.7	336.5	332.8	332.7	2 - 1	23.7-35.6	32.7
17500	336.0	336.3	(?)	(?)	(?)	2 - 1	36.9-55.3	42.5

[a] Temperature in K of segregation on crystallization from solution in higher mass PEO (from ref 4 and 5). [b] Crossover temperature in K of $\Delta G_n/(kT)$ curves for m and $m-1$ (see also Figures 2 and 3). [c] Lowest temperature in K for crystal growth with m folds (corresponds to the minimum of $\Delta G_n/(kT)$ for crystals with $(m+1)$ folds; see Figures 2 and 3). [d] Number of folds on segregation at T_c^*(I,II); l_c indicates their range of lamellar thickness in nm. [e] l is the lamellar thickness in nm of crystals with NIF at T_c^*(I,II). The solvent effect on the thermodynamic temperatures has been taken into account for the binary PEO mixtures (see ref 4).

minimum in $\Delta G_n/(kT)$ at $T_c(m-1)$ represents thus the condition of most perfection of the m-times folded molecular nucleus, and that the same time the condition of least perfection of the $(m-1)$-times folded molecular nucleus. The minimum in $\Delta G_n/(kT)$ is thus linked to the perfection of the molecular nucleus. At decreasing supercooling, the time for nucleation of a given fold number increases and the perfection of the nucleus increases, causing the decrease in $\Delta G_n/(kT)$, the molecular length dependent part of the critical nucleation barrier. The molecular mass independent part of the critical nucleation barrier provides the increased time due to its continuous increase toward a maximum.

Quantitatively the difference between $T_m(m)$ and $T_c(m-1)$ is almost molecular mass independent. For nine fractions of MW 3000–11 250 $T_m(1) - T_c(0)$ is 0.9 K, $T_m(2) - T_c(1)$ is 1.4 K, and $T_m(3) - T_c(2)$ is 2.2 K. These temperature differences are measures of crystal perfection after nucleation.

Experimental Evidence for Segregation of Molecules of Different Mass

The experimental observation of segregation of different mass molecules on crystallization is the central evidence for molecular nucleation.[1-6] Full segregation of a molecule of given mass occurs above the temperature T^*(I,II), in crystallization region I. In this high-temperature region only the high molecular mass species crystallize. In crystallization region II, at intermediate temperature, there is increasing cocrystallization as the temperature decreases. Below T^*(II,III), finally, in crystallization region III, cocrystallization is complete. Such segregation behavior could be followed experimentally to a molecular mass of up to 20 000 for the rejected low molecular mass components.[1,4] The values of T_c^*(I,II) for PEO are reproduced in the second column of Table II. A further analysis of these temperatures is possible in conjunction with the crystal growth kinetics just discussed.

Figure 3 illustrates $\Delta G_n/(kT)$, the molecular mass dependent part of the free enthalpy barrier opposing crystal growth, for the five fractions of known segregation behavior.[4,5,36] Except for the 3500 MW sample, T_c^*(I,II) is found in the vicinity of the crossover temperature of $\Delta G_n/(kT)$ of two specific fold lengths, T_c^* (see Table II). With the information in Figure 3 and Table II one can judge how many folds are involved in crystal growth at the segregation temperature T_c^*(I,II). The molecular mass 3500 must clearly involve extended-chain crystals. For the molecular masses 4640 and 7000, T_c^*(I,II) falls into the region of possible growth of once-folded or extended-chain crystals. For MW 9230, 11 250, and possibly also 17 500, T_c^*(I,II) is in the region of change from twice-folded to once-folded molecules.

To answer the question why T_c^*(I,II) occurs at the local maximum in $\Delta G_n/(kT)$ rather than at the minimum and to decide the actual number of folds of the molecular nucleus, one needs to remember that thicker lamellae do not grow on thinner lamellae without considerable decrease of growth rate.[4,6,9,11] A much higher free enthalpy barrier than indicated in Figure 2 and 3 would have to be overcome if the growing crystal layer were thicker than the substrate. No such difficulty exists for a layer thinner than the substrate. By comparison of the fold length of the high molecular mass NIF component at T_c^*(I,II) listed in column 9 of Table II which is the substrate for growth of the low molecular mass species characterized by the data of column 8, it must be concluded that the fold number of the molecular nucleus m^* is always the larger of the two listed in column 7 of Table I. The lower fold number would lead to a thicker low-MW growth than the high-MW substrate. It would then need a higher $\Delta G_n/(kT)$, and crystal growth would be much slower than for the higher fold number. The specific fold number for the molecular nucleus m^* is thus determined by the fold length of the substrate and falls in the temperature range where $\Delta G_n/(kT)$ increases rapidly with temperature. The closeness of T_c^* and T_c^*(I,II) is most likely accidental because both temperatures must fall in the range of steep $\Delta G_n/(kT)$ increase. For $m^* = 0$ the closeness of T_c^* and T_c^*(I,II) cannot, and does not, hold since there is no minimum in $\Delta G_n/(kT)$.

Figure 4 summarizes the free enthalpy barriers at T_c^*(I,II). For all nucleation paths there is a perfection after nucleation, indicated by the dashed lines. Its magnitude was discussed in the prior section. This perfection does not affect the segregation behavior but causes T_c^*(I,II) to fall below the zero-entropy-production melting temperature $T_m(m^*)$. Molecules of m^*+1 and m^*-1 folds can not grow at T_c^*(I,II): the former because of being above $T_m(m^*+1)$; the latter because of exceeding the substrate thickness. For full local thermodynamic reversibility, T_c^*(I,II) would have to coincide with $T_m(m^*)$. Since this is not so, molecular nucleation, which must involve the full chain length, is reversible only up to the end of the drawn-out part of the ΔG curve. The high efficiency of segregation suggests that the time to traverse the dashed-line portions of the ΔG curves takes longer than for an equivalent part of the drawn-out curve.

General Description of Crystal Growth of Macromolecules

To fit the just-presented observations into an overall picture, it is useful to outline the possible paths of a macromolecule from the melt to the crystal. Both the initial and final equilibrium states are thermodynamically fully known by extrapolation of equilibrium melt properties to T_c and by extrapolation of partial crystallization and perfection to equilibrium crystallinity. On crystallization, the macromolecule adjusts itself gradually from a

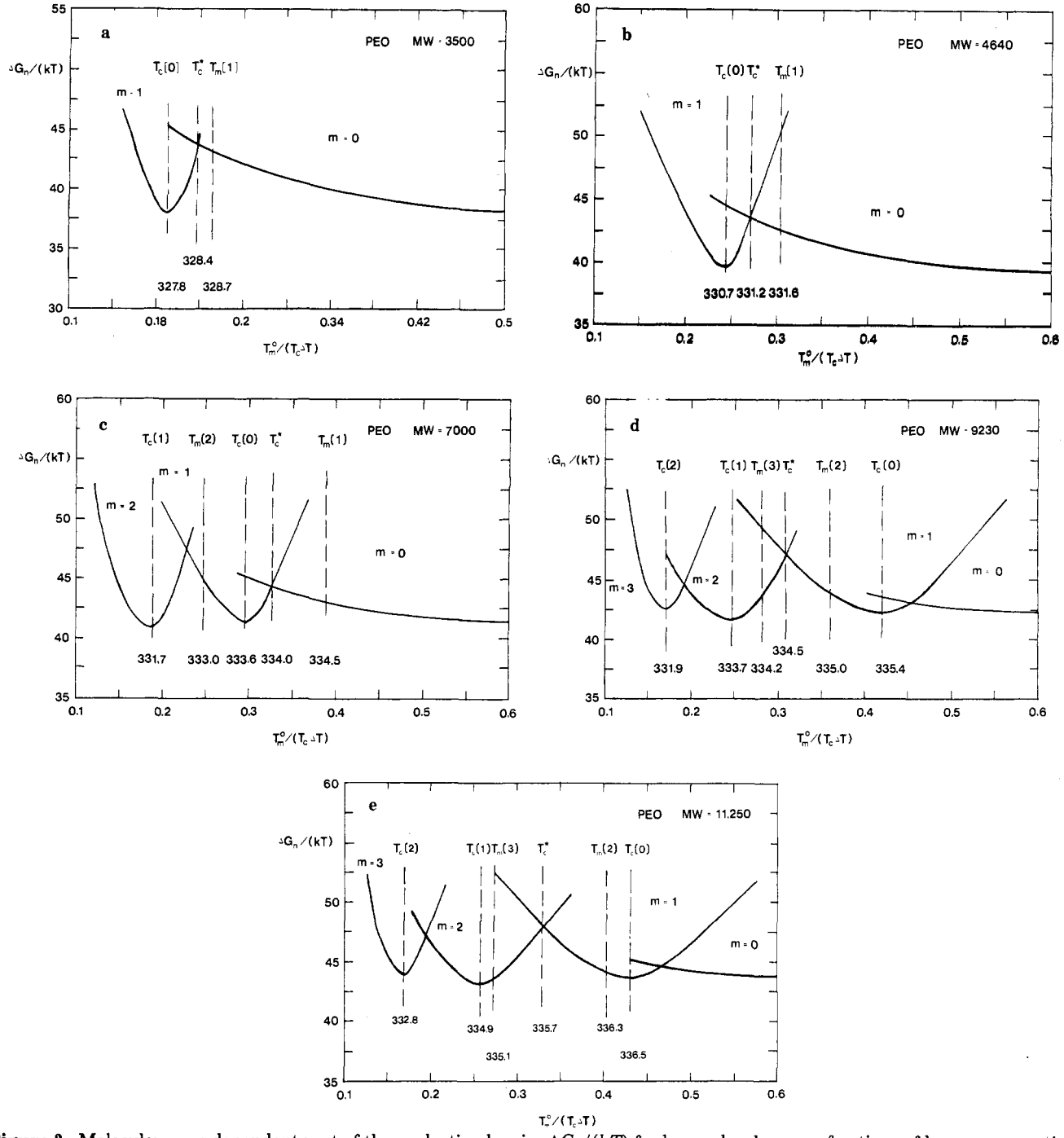

Figure 3. Molecular mass dependent part of the nucleation barrier $\Delta G_n/(kT)$ for low molecular mass fractions of known segregation behavior from solutions with 100 000 MW PEO. Data of ref 4, 5, and 36.

three-dimensional random coil in the melt to a more ordered macroconformation in two-dimensional or limited three-dimensional space. The governing thermodynamic forces are attraction of the molecule to the interface and incorporation into the crystal, opposed by the loss of entropy for these steps. Rather than going to completion, the crystallization of a macromolecule stops usually at some metastable, intermediate state of partial crystallization. One may recognize perhaps the following seven overlapping processes and their reversals: (1) primary nucleation/melting; (2) diffusion to/from the interface; (3) disentanglement/entanglement; (4) absorption/desorption; (5a) surface nucleation/surface melting; (5b) molecular nucleation/rejection; (6) crystal growth/melting; (7) crystal perfection/melting.

Process 1 has been widely studied.[37] It governs the number and thus, indirectly, the sizes of crystals or crystal superstructures (i.e., spherulites). In the present discussion its effect is eliminated by providing for heterogeneous nucleation. Processes 2–4 will be simplified for the present discussion and collectively described by a diffusion rate v_D. The importance of process 3 is demonstrated, for example, by the well-known decrease in crystallinity when molecular mass is sufficiently long not to permit complete disentanglement. Of special importance to the present discussion are the processes 5–7. Steps 5 are described by the surface and molecular nucleation rates i, process 6 by the lateral crystal growth rate v_g, and process 7 by some perfection rate v_p. All 12 possible combinations of these four rates are listed in Table III with short characterizations.

Starting with crystallization at high supercooling (types 9 to 12) one should, in the limit, reach "cold crystallization",[38] a solidification type also represented by

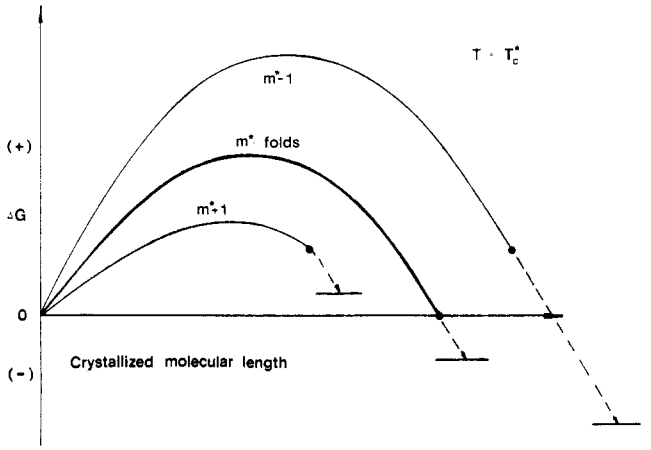

Figure 4. Schematic free enthalpy diagram of the nucleation segregation process at T_c^*(I,II). Crystallization occurs only for crystals with m^* folds. This substrate thickness is about the same as that of m^*-folded chain crystals. The dashed lines represent the perfection after nucleation, to be discussed below. Crystals with $m^* + 1$ folds are above their $T_m(m^* + 1)$ (see Figure 3).

Table III
Possible Types of Crystal Growths from the Melt

$v_D > i$		single lamellar crystal growth and maximum adjustment of macroconformation crystal morphology
A	$i > v_g$	overlapping nucleation and growth
1	$v_g < v_p$	perfection during growth
2	$v_g > v_p$	perfection after growth
B	$i < v_g$	nucleation controlled growth
3	$v_g < v_p$	perfection during growth
4	$v_g > v_p$	perfection after growth
$v_D \approx i$		polycrystalline growth with limited adjustment of macroconformation to crystal morphology
C	$i > v_g$	overlapping nucleation and growth
5	$v_g < v_p$	perfection during growth
6	$v_g > v_p$	perfection after growth
D	$i < v_g$	nucleation controlled growth
7	$v_g < v_p$	perfection during growth
8	$v_g > v_p$	perfection after growth
$v_D < i$		cold crystallization without adjustment of macroconformation to crystal morphology
E	$i > v_g$	overlapping nucleation and growth
9	$v_g < v_p$	perfection during growth
10	$v_g > v_p$	perfection after growth
F	$i < v_g$	nucleation controlled growth
11	$v_g < v_p$	perfection during growth
12	$v_g > v_p$	perfection after growth

the "Erstarrungsmodell".[39] In such crystallization small-angle neutron scattering showed no change of the radius of gyration of the molecule on going from the melt to the semicrystalline state.[39,40] Small, metastable crystals produced by minimal translational and rotational motion of the repeating units are expected under such conditions. The actual length of the molecule becomes unimportant in this limiting case of crystallization. Indeed, the constant *A* of eq 1 approaches zero at high supercooling (see Table I). The linear crystal growth rate v_c exceeds 10^4 nm/s, which corresponds to a growth of the same order of magnitude of crystal layers per second (see Figure 1). Figure 5 shows that a true independence of crystallization on molecular mass is reached at $1/\Delta T = 0.00735$ or $\Delta T = 136$ or $T_c = 342–136$ K = 206 K. This temperature is, as expected, the glass transition temperature of PEO.[15]

Decreasing the supercooling, one finds from Figure 1 no abrupt change in mechanism. One may thus try to perhaps link eq 1 and 2 with the classical nucleation theory as one approaches crystallization types 5–8 of Table III. Let us

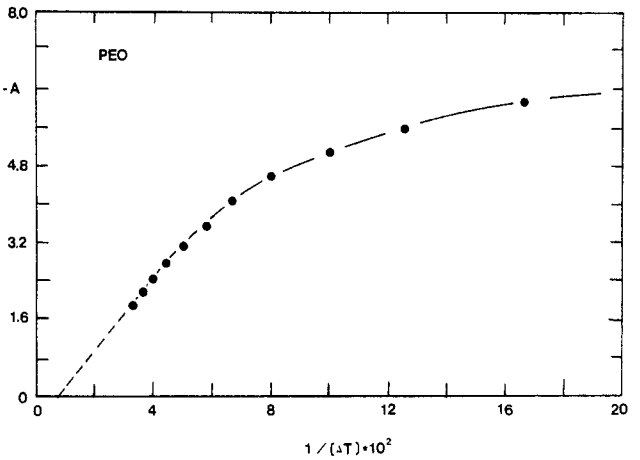

Figure 5. Relationship between the molecular mass dependent term *A* of eq 1 and $1/\Delta T$ in the high supercooling range.

assume one can write for the molecular mass independent part

$$B = \log v_0 - 0.434\Delta G_\eta/(kT) \quad (3)$$

i.e., *B* represents the product of the preexponential factor of the classical nucleation theory ($v_0 = bkT/h$, where *b* is the thickness of one crystal layer and *h* is Planck's constant) and the term accounting for the hindering of motion across the phase boundary (free enthalpy barrier ΔG_η). For $\Delta G_\eta/(kT)$ one usually applies the universal WLF equation $2070/(51.6 + T - T_g)$ where T_g is the glass transition temperature (206 K).[15] An experimentally derived equation from melt viscosity $\Delta G_\eta/(kT) = 3530/T$ is only little different from the WLF equation.[10] Calculated values for *B* with the crystallographic $b = 0.656$ nm at 300, 310, 320, and 330 K are 6.44, 6.86, 7.22, and 7.54 for the WLF estimate, and 7.50, 7.69, 7.85, and 8.01 for the melt viscosity estimate, respectively. These values are close enough in magnitude and supercooling trend to suggest that *B* is in this supercooling range well represented by the interpretation of eq 3. Turning to *A* in this range of intermediate supercooling, Figure 5 shows that its dependence can over narrow ranges of supercooling be fit to a linear $1/\Delta T$ dependence,[5] the broad range appearance is, however, neither that of one nor of two or three linear segments, as required by the classical theory. The double-logarithmic dependence of v_c on chain length *n* suggests a cooperative crystallization process (see eq 1a). Our attempts to derive a simple model that would lead to such a rate law have up to now not been successful. As a different approach we are at present attempting to simulate nucleation and crystallization processes by Monte Carlo and molecular dynamics simulations.[7]

Decreasing the supercooling further, one approaches the cases 1–4 of Table III. The major difference is the much slower crystallization; i.e., there is more time for perfection during and after nucleation, while in the higher supercooling cases major perfection occurs under analogous conditions more often after crystallization.

For PEO integral folding, IF becomes in this temperature range more efficient than NIF (see Figure 1). The change of NIF to IF and the successive changes in fold number *m* lead to discontinuities in v_c and major jumps in *A* and *B* (see Table I). The parameter *A* changes by a factor of 4–6 and *B* by a factor of 3–5, making the prior interpretations untenable. Both v_0 and ΔG_η as computed above are changing only slowly in the rather narrow temperature range of IF. The value of *B* for IF is so large that even a zero value for ΔG_η is not sufficient to account for

the experimental data in Table I ($\log v_0 = 12.7$ at 340 K). If one wants to stay within the framework of classical nucleation theory one must assume that all three parts contributing to crystal growth, frequency factor, viscosity form, and nucleation barrier are molecular mass dependent. As indicated above, such crystallization behavior seems at present only to be amenable to computer simulation.

Conclusions

A number of experiments point to the need to incorporate the description of molecular mass dependent, cooperative processes into the model for crystallization of macromolecules. It seems best outlined by the sequence primary nucleation followed sometimes by surface nucleation and always governed by molecules nucleation, followed by crystal growth. All of these steps in crystallization must be analyzed considering nucleus or crystal perfection during and after the processes and freezing before thermodynamic equilibrium is reached. Computer simulation seems the best future technique to get further insight into the crystallization of macromolecules.

Acknowledgment. This work was supported by Grant DMR 83-17097 of the Polymers Program, Division of Materials Research of the National Science Foundation. We also appreciate recent communications with Professors J. D. Hoffman and R. L. Miller of Midland Molecular Institute. Considerable insight has been gained from extensive discussions with them. At ORNL the work was sponsored by the Division of Materials Science, Office of Basic Energy Sciences, U.S. Department of Energy, under Contract DE-AC05-840R21400 with Martin Marietta Energy Systems Inc.

Temperature Definitions

T	temperature in kelvin
T_c	crystallization temperature
T_{in}	temperature of shift from low-temperature, nonintegral to high-temperature, integral chain folding on crystallization
$T_m(0)$	equilibrium melting temperature (extended chain crystal of given mass with zero folds)
T_m^0	equilibrium melting temperature of extended chain crystals of infinite mass
$T_m(m)$	zero entropy production melting temperature of a crystal containing m-times regularly folded molecules of given mass (local equilibrium, no change in metastability on fusion)
ΔT	supercooling $[T_m(m) - T]$
$T_c(m)$	lowest temperature at which for a given molecular mass crystallization occurs with m-times folded molecules
T_c^*	crossover of ΔG_n curves for m- and $(m + 1)$-times folded molecules, where n is the degree of polymerization and ΔG_n is the free enthalpy of nucleation of a molecule of given n and m
T_c^*(I,II)	lowest temperature for complete segregation of a given low molecular mass molecule on crystallization from solution in a given high molecular mass solvent (temperature separating crystallization regions I and II, see ref 4–6)
T_c^*(II,-III)	highest temperature for complete cocrystallization of a solution of given low and high molecular mass (temperature separating crystallization regions III and II, see ref 4–6)

Registry No. PEO, 25322-68-3.

References and Notes

(1) Wunderlich, B.; Mehta, A. *J. Polym. Sci., Polym. Phys. Ed.* **1974**, *12*, 255.
(2) Mehta, A.; Wunderlich, B. *Colloid Polym. Sci.* **1975**, *253*, 193.
(3) Wunderlich, B. *Faraday Discuss. Chem. Soc.* **1979**, *No. 68*, 239.
(4) Cheng, S. Z. D.; Wunderlich, B. *J. Polym. Sci., Part B Phys. Ed.* **1986**, *24*, 577.
(5) Cheng, S. Z. D.; Wunderlich, B. *J. Polym. Sci., Part B: Phys. Ed.* **1986**, *24*, 595.
(6) Cheng, S. Z. D.; Bu, H. S.; Wunderlich, B. *J. Polym. Sci., Part B: Phys. Ed.* **1988**, *26*, 1947.
(7) Noid, D. W.; Pfeffer, G. A.; Cheng, S. Z. D.; Wunderlich, B. *Macromolecules*, in press.
(8) Kovacs, A. J.; Gonthier, A. *Kolloid Z. Z. Polym.* **1972**, *250*, 530.
(9) Kovacs, A. J.; Gonthier, A.; Straupe, C. *J. Polym. Sci., Polym. Symp.* **1975**, *No. 50*, 283.
(10) Kovacs, A. J.; Straupe, C.; Gonthier, A. *J. Polym. Sci., Polym. Symp.* **1977**, *No. 59*, 31.
(11) Kovacs, A. J.; Straupe, C. *Faraday Discuss. Chem. Soc.* **1979**, *No. 68*, 225.
(12) Kovacs, A. J.; Straupe, C. *J. Cryst. Growth* **1980**, *48*, 210.
(13) Grebowicz, J.; Suzuki, H.; Wunderlich, B. *Polymer* **1985**, *26*, 561.
(14) Suzuki, H.; Grebowicz, J.; Wunderlich, B. *Makromol. Chem.* **1985**, *189*, 1109.
(15) Suzuki, H.; Wunderlich, B. *J. Polym. Sci., Polym. Phys. Ed.* **1985**, *23*, 1671.
(16) Buckley, C. P.; Kovacs, A. J. *Prog. Colloid Polym. Sci.* **1975**, *44*; *Kolloid Z. Z. Polym.* **1976**, *254*, 659.
(17) Lauritzen, J. I., Jr.; Hoffman, J. D. *J. Chem. Phys.* **1959**, *31*, 1680.
(18) Hoffman, J. D.; Lauritzen, J. I., Jr. *J. Res. Natl. Bur. Stand., Sect. A* **1961**, *A65*, 297.
(19) Frank, F. C.; Tosi, M. *Proc. R. Soc. London* **1961**, *A263*, 323.
(20) Price, F. P. Nucleations in polymer crystallization. In *Nucleation*; Zettlemoyer, A. E., Ed.; Dekker: New York, 1969.
(21) For an earlier review, see for example: Wunderlich, B. *Macromolecular Physics, Crystal Nucleation, Growth, Annealing*; Academic Press: New York, 1976; Vol. 2.
(22) Frank, F. C. *J. Cryst. Growth* **1974**, *22*, 233.
(23) Sanchez, J. C.; DiMarzio, E. A. *J. Res. Natl. Bur. Stand., Sect. A* **1972**, *A76*, 213.
(24) Lauritzen, J. I., Jr.; Hoffman, J. D. *J. Appl. Phys.* **1973**, *44*, 4340. Lauritzen, J. I., Jr. *J. Appl. Phys.* **1973**, *44*, 4353.
(25) Hoffman, J. D.; Frolen, L. J.; Ross, G. S.; Lauritzen, J. I., Jr. *J. Res. Natl. Bur. Stand., Sect. A* **1975**, *79A*, 671.
(26) Hoffman, J. D.; Guttman, C. M.; DiMarzio, E. A. *Faraday Discuss. Chem. Soc.* **1979**, *No. 68*, 177.
(27) Hoffman, J. D. *Polymer* **1982**, *23*, 656. See also: *Polymer* **1983**, *24*, 3.
(28) Point, J. J.; Kovacs, A. J. *Macromolecules* **1980**, *13*, 399.
(29) Hoffman, J. D. *Macromolecules* **1986**, *19*, 1124.
(30) Sadler, D. M. *J. Polym. Sci., Polym. Phys. Ed.* **1985**, *23*, 1533.
(31) Wunderlich, B.; Melillo, L.; Cormier, C. M.; Davidson, T.; Synder, G. *J. Macromol. Sci., Phys.* **1967**, *B1*, 485.
(32) Wunderlich, B.; Cormier, C. M. *J. Phys. Chem.* **1966**, *70*, 1844.
(33) Wunderlich, B.; Cheng, S. Z. D. *Gazz. Chim. Ital.* **1986**, *116*, 345.
(34) Wunderlich, B.; Shu, H.-C. *J. Cryst. Growth* **1980**, *48*, 227.
(35) (a) Hoffman, J. D. *Polymer*, **1985**, *26*, 803. (b) In a private communication it was suggested by J. D. Hoffman that these values may be only in an upper limit of 20 nm, about $^1/_{35}$th of the quoted ones.
(36) Cheng, S. Z. D. Ph.D. Thesis, Department of Chemistry, Rensselaer Polytechnic Institute, Troy, NY 12180-3590, 1985. See also recent, unpublished, more detailed work in the low supercooling range for some low molecular mass fractions.
(37) For nucleation theory, see: Glasstone, S.; Laidler, K. L.; Eyring, H. *The Theory of Rate Processes*; McGraw-Hill: New York, 1941. Turnbull, D.; Fisher, J. C. *J. Chem. Phys.* **1949**, *17*, 71. For application to polymer primary nucleation, see ref 17–27.
(38) Wunderlich, B. *J. Chem. Phys.* **1958**, *29*, 1395.
(39) Fischer, E. W. *Pure Appl. Chem.* **1978**, *50*, 1319.
(40) Sadler, D. M.; Keller, A. *Macromolecules* **1977**, *10*, 1128.